Int. J. Electrochem. Sci., 9 **(2014)** 6852 - 6857

International Journal of ELECTROCHEMICAL SCIENCE
www.electrochemsci.org

Short Communication

Distinct Effect of Cooling Rate on Structure and Electrochemical Performance of Lithium Rich Layered Oxides: a Case Study of $0.3Li_2MnO_3 \cdot 0.7LiNi_{0.5}Mn_{0.5}O_2$

Fushan Feng, Haisheng Fang[*]*, Bin Yang, Wenhui Ma, Yongnian Dai*

State Key Laboratory of Complex Nonferrous Metal Resources Clear Utilization, Kunming University of Science and Technology, Kunming 650093, China
Key Laboratory of Nonferrous Metals Vacuum Metallurgy of Yunnan Province, Kunming University of Science and Technology, Kunming 650093, China
Faculty of Metallurgical and Energy Engineering, Kunming University of Science and Technology, Kunming 650093, China
[*]E-mail: hsfang1981@hotmail.com

Received: 1 August 2014 / *Accepted:* 8 September 2014 / *Published:* 29 September 2014

$0.3Li_2MnO_3 \cdot 0.7LiNi_{0.5}Mn_{0.5}O_2$ is prepared by a solid-state method with a two-step heating process, and the effect of cooling rate after the first-step heating on structure and electrochemical behavior of the obtained material is studied. The result shows that the sample prepared with a slow cooling has much better electrochemical performance due to its better structural integration between Li_2MnO_3 and $LiNi_{0.5}Mn_{0.5}O_2$ than the sample obtained with a quick cooling. Such an effect of cooling rate after the first-step heating in our work is contrary to the effect of cooling rate after the second-step heating as previously reported.

Keywords: Lithium ion batteries; Cathode material; Li-rich layered oxide; Cooling rate

1. INTRODUCTION

Li-rich layered oxides have attracted great attention as promising cathode materials for lithium ion batteries because they can deliver much higher capacities (~ 250 mAh g^{-1}) [1-7]. These oxides may be thought of as composite materials denoted as $xLi_2MnO_3 \cdot (1-x)LiMO_2$ ($0 < x < 1$, M = Mn, Ni, Co, etc.) which are composed of a trigonal $LiMO_2$ phase (space group R-3m) and a monoclinic Li_2MnO_3 phase (space group C2/m) [1-4], and the structural integration of Li_2MnO_3 with $LiMO_2$ is essential to achieve high performance $xLi_2MnO_3 \cdot (1-x)LiMO_2$ [8]. Based on the available literature [8, 9], it is known that the structural integration of a specific Li-rich layered oxide is highly dependent on the

synthesis method and condition. To obtain high quality Li-rich layered oxides, it is extremely important to know what synthesis parameters are likely to affect the structural integration between Li_2MnO_3 and $LiMO_2$. Previous work has reported that cooling rate may sometimes greatly affect structure and electrochemical performance of the obtained Li-rich layered oxides [9, 10], but attention was only focused on the cooling rate after the final heating process [9-11]. Currently, a two-step heating process has been widely adopted to synthesize $xLi_2MnO_3 \cdot (1-x)LiMO_2$ [8-12], but effect of cooling rate after the first-step heating remains uncovered.

In the present work, two $0.3Li_2MnO_3 \cdot 0.7LiNi_{0.5}Mn_{0.5}O_2$ samples are prepared by a solid-state method with a two-step heating process, and the effect of cooling rate after the first-step heating on structure and electrochemical behavior of the obtained materials is preliminarily investigated. The results show that the cooling rate after the first-step heating exerts a big influence on structure and electrochemical performance of the obtained $0.3Li_2MnO_3 \cdot 0.7LiNi_{0.5}Mn_{0.5}O_2$, but has the opposite effect from the cooling rate after the second-step heating as previously reported [9].

2. EXPERIMENTAL

$0.3Li_2MnO_3 \cdot 0.7LiNi_{0.5}Mn_{0.5}O_2$ materials were prepared by a solid-state method with a two-step heating process. Chemicals of Li_2CO_3, $MnCO_3$ and $NiCO_3 \cdot 2Ni(OH)_2 \cdot 4H_2O$ with a stoichiometric amount were fully mixed with deionized water by ball-milling for 5 h and dried overnight at 90 ^oC in a vacuum oven. The obtained precursor was firstly heated at 400 ^oC for 5 h in muffle furnace and then cooled to room temperature with two different ways: (1) natural cooling (slow cooling) in muffle furnace, or (2) quenched (quick cooling) out of muffle furnace in air. The cooled powders were well grounded in an agate mortar and then heated at 900 ^oC for 20 h in muffle furnace followed by a natrual cooling in muffle furnace. The heating rate was fixed at 5 $^oC\ min^{-1}$ for both steps of heating.

The crystalline phase of the obtained materials was identified by X-ray diffraction (XRD, D/MaX-3B, Rigaku). Raman spectroscopy was measured using a Reinshaw inVia Raman microscope at room temperature with an Ar 514.5 nm laser as excitation source. Materials morphology and particle size were observed by scanning electron microscopy (SEM, XL30, Philips).

Electrochemical properties were assessed using CR2025 coin cells with a lithium metal anode. The cathode was made by mixing active material, super P and polyvinylidene fluoride (PVDF) in a weight ratio of 8:1:1 in N-methyl pyrrolidinone (NMP) to form homogenous slurry. Then the slurry was coated on an aluminium foil by a doctor blade coater and dried in a vacuum oven. The electrolyte was 1 M $LiPF_6$ in EC/DMC(1/1 in volume) solution. All cells were assembled in an Ar-filled glove box. Cells were charged and discharged between 2.0 and 4.8 V using a battery test system (Land CT2001A) at 30 ^oC.

3. RESULTS AND DISSCUSSION

Figure 1 shows XRD patterns of the two $0.3Li_2MnO_3 \cdot 0.7LiNi_{0.5}Mn_{0.5}O_2$ samples obtained with different cooling ways after the first-step heating. All peaks of the two patterns can be indexed on the

basis of two layer structures: the trigonal (T) $LiNi_{0.5}Mn_{0.5}O_2$ phase and the monoclinic (M) Li_2MnO_3 phase. The weak reflections in the 2θ range of ~20º-25º are characteristic of the monoclinic structure of the Li_2MnO_3 phase [4]. However, there is an obvious difference between the two patterns. The $(101)_T/(104)_T$ peaks of the $LiNi_{0.5}Mn_{0.5}O_2$ phase in the 2θ range of 35 to 45º are clearly separated from the $(111)_M/(131)_M$ peaks of the Li_2MnO_3 phase for the sample obtained with a quick cooling (Figure 1b), while these peaks of the two phases are almost integrated into two peaks for the sample obtained with a slow cooling (Figure 1a). The same phenomenon is observed in the 2θ range of 62 to 70º. These observations demonstrate that the structure of $0.3Li_2MnO_3 \cdot 0.7LiNi_{0.5}Mn_{0.5}O_2$ is highly sensitive to the cooling rate after the first-step heating. A quick cooling may lead to the phase separation of Li_2MnO_3 and $LiNi_{0.5}Mn_{0.5}O_2$ while a slow cooling is beneficial to form structurally integrated layered composition.

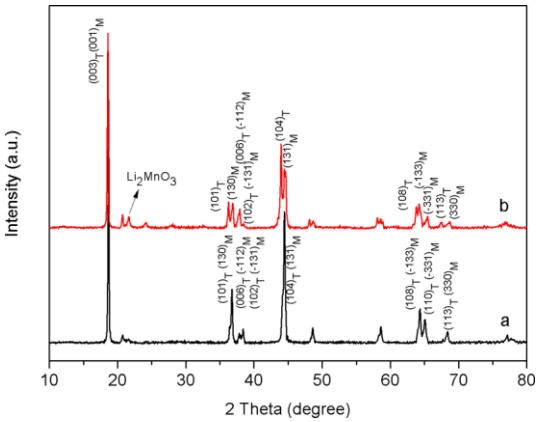

Figure 1. XRD patterns of the two $0.3Li_2MnO_3 \cdot 0.7LiNi_{0.5}Mn_{0.5}O_2$ samples obtained with different cooling ways after the first-step heating: (a) slow cooling and (b) quick cooling.

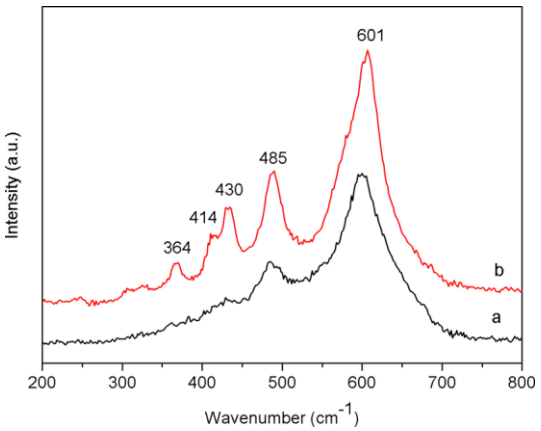

Figure 2. Raman spectra of the two $0.3Li_2MnO_3 \cdot 0.7LiNi_{0.5}Mn_{0.5}O_2$ samples obtained with different cooling ways after the first-step heating: (a) slow cooling and (b) quick cooling

Figure 2 shows Raman spectra of the two $0.3Li_2MnO_3 \cdot 0.7LiNi_{0.5}Mn_{0.5}O_2$ samples obtained with different cooling ways after the first-step heating. The sample obtained with a slow cooling has

three peaks at 601, 485 and 430 cm^{-1} (Figure 2a), which is in agreement with the previous studies on Li-rich layered oxides [13,14], indicating a fine integration of $0.3Li_2MnO_3 \cdot 0.7LiNi_{0.5}Mn_{0.5}O_2$. However, there are two more peaks at 414 and 364 cm^{-1} observed for the sample obtained with a quick cooling (Figure 2b) which are only associated with the individual Li_2MnO_3 [15,16], suggesting that the Li_2MnO_3 phase did not structurally integrate with the $LiNi_{0.5}Mn_{0.5}O_2$ phase. Namely, the sample obtained with a slow cooling has much better integration of the Li_2MnO_3 with the $LiNi_{0.5}Mn_{0.5}O_2$ than the sample obtained with a quick cooling. This result is well consistent with the above XRD study. In addition, the morphology and particle size of the two $0.3Li_2MnO_3 \cdot 0.7LiNi_{0.5}Mn_{0.5}O_2$ samples were measured by SEM as shown in Figure 3 and no obvious difference was observed. Therefore, the cooling way after the first-step heating only affects the structure of $0.3Li_2MnO_3 \cdot 0.7LiNi_{0.5}Mn_{0.5}O_2$ but not the morphology and particle size.

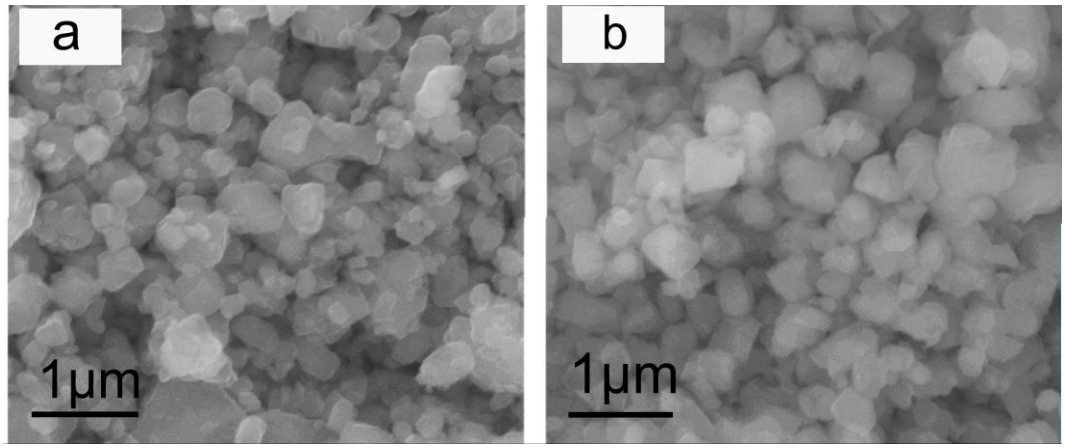

Figure 3. SEM images of the two $0.3Li_2MnO_3 \cdot 0.7LiNi_{0.5}Mn_{0.5}O_2$ samples obtained with different cooling ways after the first-step heating: (a) slow cooling and (b) quick cooling.

Figure 4 (left) shows the initial charge/discharge curves of the two $0.3Li_2MnO_3 \cdot 0.7LiNi_{0.5}Mn_{0.5}O_2$ samples obtained with different cooling ways after the first-step heating. Cells were cycled at 0.1 C (1 C is equal to 250 mA g^{-1}) between 2.0 and 4.8 V. Clearly, completely different electrochemical behavior is observed for the two samples. For the sample obtained with a slow cooling, the initial charge curve exhibits a two-plateau profile. The voltage plateau above 4.5 V is the characteristic feature of the integrated $xLi_2MnO_3 \cdot (1\text{-}x)LiNi_{0.5}Mn_{0.5}O_2$, and can be attributed to the simultaneous removal of lithium and oxygen from the Li_2MnO_3 component [4,17]. The initial charge and discharge capacities are 251 and 172 mAh g^{-1}, respectively. For the sample obtained with a quick cooling, however, only a reversible capacity of 38 mAh g^{-1} is observed, and the charge plateau above 4.5 V is absent, indicating that the Li_2MnO_3 phase is not activated. Figure 4 (right) shows the rate performance of the two $0.3Li_2MnO_3 \cdot 0.7LiNi_{0.5}Mn_{0.5}O_2$ samples. Cells were charged at 0.1C to 4.8 V and then discharged at various rates to 2.0 V. The sample obtained with a slow cooling has much higher discharge capacities at all rates as compared to that obtained with a quick cooling. However, we should point out that although the sample obtained with a slow cooling

possesses better performance, the reversible capacity is still not high, which may be due to two factors: (1) the structural integration between Li_2MnO_3 and $LiNi_{0.5}Mn_{0.5}O_2$ is still not perfect and (2) the particle size is relatively large. Enhanced electrochemical performance may be achieved by improvement of structural integration and particle size reduction through optimizing ball-milling and calcination conditions.

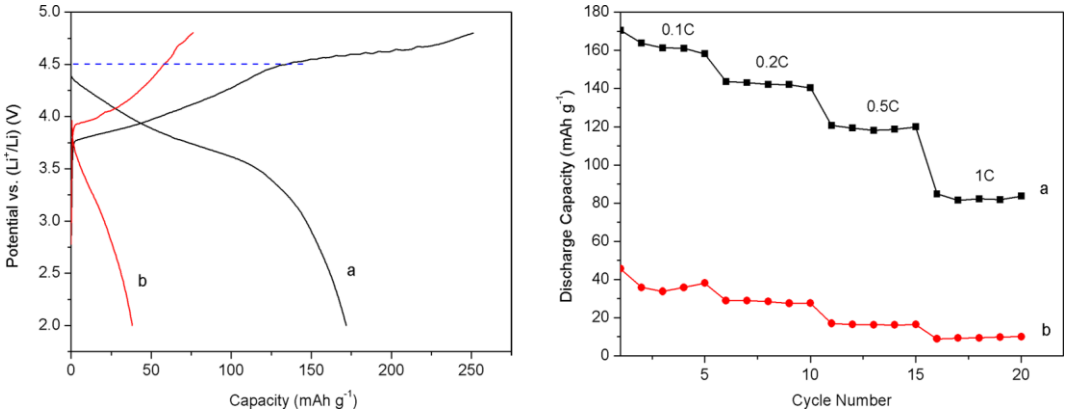

Figure 4. (Left) The initial charge/discharge curves of the two $0.3Li_2MnO_3 \cdot 0.7LiNi_{0.5}Mn_{0.5}O_2$ samples obtained with different cooling ways after the first-step heating: (a) slow cooling and (b) quick cooling. Cells were cycled at 0.1C between 2.0 and 4.8 V. (Right) Rate performance of the two $0.3Li_2MnO_3 \cdot 0.7LiNi_{0.5}Mn_{0.5}O_2$ samples obtained with different cooling ways after the first-step heating: (a) slow cooling and (b) quick cooling. Cells were charged at 0.1C to 4.8 V and then discharged at various rates to 2.0 V.

From the above measurements, we can conclude that the sample obtained with a slow cooling has much better electrochemical performance due to its better structural integration than the sample obtained with a quick cooling. As compared the present work with the previous report [9], it is interesting that the effect of cooling rate after the first-step heating is directly opposite to that after the second-step heating. This demonstrates that the same process parameter at different processing step may have a completely different effect on Li-rich layered oxides.

4. CONCLUSIONS

Two $0.3Li_2MnO_3 \cdot 0.7LiNi_{0.5}Mn_{0.5}O_2$ samples have been synthesized by a two-step heating process, and the cooling rate after the first-step heating at 400 ^oC was shown to have a significant impact on the structure and electrochemical behavior. A quick cooling after the first-step heating led to the phase separation between Li_2MnO_3 and $LiNi_{0.5}Mn_{0.5}O_2$ in the obtained material, and as a result poor electrochemical performance was observed. However, a slow cooling after the first-step heating yielded well integrated $0.3Li_2MnO_3 \cdot 0.7LiNi_{0.5}Mn_{0.5}O_2$, and consequently much better electrochemical performance could be achieved. These observations demonstrate that the cooling rate after the first-step heating has the opposite effect from that after the second-step heating as previously reported.

These findings are fundamentally important to rationally and controllably synthesize high performance Li-rich layered oxides.

ACKNOWLEDGEMENTS
This work was supported by the National Natural Science Foundation of China (No. 51304098), the Specialized Research Fund for the Doctoral Program of Higher Education (No.20125314120004), the Program for Innovative Research Team in University of Ministry of Education of China (No. IRT1250) and the Academician Exploration Program of Yunnan province (2013HA011).

References

1. C.S. Johnson, J.S. Kim, C. Lefief, N. Li, J.T. Vaughey, and M.M. Thackeray, *Electrochem. Commun.*, 6 (2004) 1085.
2. M.M. Thackeray, C.S. Johnson, J.T. Vaughey, N. Li, and S.A. Hackney, *J. Mater. Chem.*, 15 (2005) 2257.
3. M.M. Thackeray, S.H. Kang, C.S. Johnson, J.T. Vaughey, and S.A. Hackney, *Electrochem. Commun.*, 8 (2006) 1531.
4. M.M. Thackeray, S.H. Kang, C.S. Johnson, J.T. Vaughey, R. Benedek, and S.A. Hackney, *J. Mater. Chem.*, 17 (2007) 3112.
5. Z.H. Lu, Z.H. Chen, and J.R. Dahn, *Chem. Mater.*, 15 (2003) 3214.
6. J. Bréger, M. Jiang, N. Dupré, Y.S. Meng, Y. Shao-Horn, G. Ceder, and C.P. Grey, *J. Solid State Chem.*, 178 (2005) 2575.
7. K. A. Jarvis, Z. Deng, L.F. Allard, A. Manthiram, and P.J. Ferreira, *Chem. Mater.*, 23 (2011) 3614.
8. C. Ghanty, S. Chatterjee, R.N. Basu, and S.B. Majumder, *J. Electrochem. Soc.*, 160 (2013) A1406.
9. S.H. Kang, and K. Amine, *J. Power Sources*, 124 (2003) 533.
10. L.Q. Zhang, K. Takada, N. Ohta, K. Fukuda, and T. Sasaki, *J. Power Sources*, 146 (2005) 598.
11. S.K. Jeong, C.H. Song, K.S. Nahm, and A.M. Stephan, *Electrochim. Acta*, 52 (2006) 885.
12. H. Koga, L. Croguennec, P. Mannessiez, M. Ménétrier, F. Weill, L. Bourgeois, M. Duttine, E. Suard, and C. Delmas, *J. Phys. Chem. C*, 116 (2012) 13497.
13. J. Hong, D.H. Seo, S.W. Kim, H. Gwon, S.T. Oh, and K. Kang, *J. Mater. Chem.*, 20 (2010) 10179.
14. F. Amalraj, M. Talianker, B. Markovsky, D. Sharon, L. Burlaka, G. Shafir, E. Zinigrad, O. Haik, D. Aurbach, J. Lampert, M. Schulz-Dobrick, and A. Garsuch, *J. Electrochem. Soc.*, 160 (2013) A324.
15. C.M. Julien, and D. Massot, *Mater. Sci. Eng. B*, 100 (2003) 69.
16. S.F. Amalraj, B. Markovsky, D. Sharon, M. Talianker, E. Zinigrad, R. Persky, O. Haik, J. Grinblat, J. Lampert, M. Schulz-Dobrick, A. Garsuch, L. Burlaka, and D. Aurbach, *Electrochim. Acta*, 78 (2012) 32.
17. A.R. Armstrong, M. Holzapfel, P. Novák, C.S. Johnson, S.H. Kang, M.M. Thackeray, and P.G. Bruce, *J. Am. Chem. Soc.*, 128 (2006) 8694.